American Journal of Science, Engineering and Technology
2023; 8(1): 33-41
http://www.sciencepublishinggroup.com/j/ajset
doi: 10.11648/j.ajset.20230801.14
ISSN: 2578-8345 (Print); ISSN: 2578-8353 (Online)

Design a Viable 3DP Processing for Producing Effective Controlled-Release Pesticide

Ben Yao[1], Zhining Xu[1], Jianan Liu[1], Liang Yang[1], Jianping Shang[1], Jingyuan Fan[2], Lizhi Ouyang[3], Hua-Jun Shawn Fan[1, *]

[1]College of Chemical Engineering, Sichuan University of Science and Engineering, Zigong, China

[2]Carnegie Vanguard High School, Houston, USA

[3]Department of Physics and Mathematics, Tennessee State University, Nashville, USA

Email address:

fan27713@yahoo.com (Hua-Jun Shawn Fan)

[*]Corresponding author

To cite this article:

Ben Yao, Zhining Xu, Jianan Liu, Liang Yang, Jianping Shang, Jingyuan Fan, Lizhi Ouyang, Hua-Jun Shawn Fan. Design a Viable 3DP Processing for Producing Effective Controlled-Release Pesticide. *American Journal of Science, Engineering and Technology*. Vol. 8, No. 1, 2023, pp. 33-41. doi: 10.11648/j.ajset.20230801.14

Received: November 14, 2022; **Accepted**: December 12, 2022; **Published**: February 16, 2023

Abstract: Various factors such as solubility, volatility, spray drift, runoff, and photolysis prevent the pesticides to reach their desired location and realize their full potential. In this study, additive manufacturing is used to create a drug-loaded filament that can be used in Fused deposition modeling printing. The optimal printing parameters are printing temperature (170°C), hotbed temperature (25°C), printing speed 15 mm/s, filament diameter 1.55 mm, layer height 0.3 mm, nozzle diameter 0.4 mm and zero retraction speed and retraction distance. The PCL-based framework provides a scaffold for drug encapsulation and low melting temperature. The latter is the key to maintaining the integrity and chemical properties of the loaded drug. FTIR confirms the physical-mix nature of composite. XRD suggests that PCL and model drug became amorphous after printing. The PCL controlled-release can be realized through *in vitro* dissolution tests. Among the four kinetic models: the zero-order, first-order, Higuchi model, and Korsmeyer–Peppas model, the kinetic model for dissolution and drug release conforms to the Korsmeyer–Peppas model. This study provides a viable design of controlled-release pesticides by adjusting the release regulator content and type to meet the precision pest-control needs. This 3DP tablet has higher drug loading, controllable drug loading, stable drug release ability, UV shielding performance, and an easy manufacturing process. There is no need for expensive and special equipment to produce the desired functionality, which greatly reduces production costs and simplifies the production process.

Keywords: 3D Printing Pesticide, Controlled-Release, Fused Deposition Modeling, Poly ε-caprolactone, Hydroxypropyl Methylcellulose

1. Introduction

Pesticides are widely used in agriculture to control weeds, diseases, and insect pests [1]. But its usage is a double edge sword. On one end, it brings huge agricultural and economic benefits by increasing production and crop yields [2]; on the other end, it also creates environmental and health hazards when misused, over-application, and other handling issues. For example, due to the poor water solubility, volatility of conventional pesticide formulations, spray drift, runoff, photolysis, and other environmental factors [3, 4], more than 50% of the pesticides applied failed to reach the target location, and the actual utilization of target organisms is less than 0.1% [5, 6]. This not only results in economic loss but also creates environmental and health hazards. In the past ten years, sustained- or controlled-release pesticide formulations have been developed to alleviate these problems. Alternative carriers for sustained-release pesticides include nanoparticles, nano-emulsions, nanocrystals, hydrogels, and various organic and inorganic nanomaterials that have been developed [7-10]. However, these nano-carriers have several disadvantages such as low loading capacity, low encapsulation efficiency, a large number of surfactants needed to obtain nano-sized oil droplets, non-biocompatibility, special equipment required,

high cost, and the decline in production efficiency [11]. Therefore, there are need to research alternative preparation of sustained-release pesticides for target-focused application, more efficient pesticide usage and more environmentally friendly application of pesticides.

As a popular additive manufacturing technology, 3D printing (3DP) is also known as incremental molding technology [12]. Its principle is to accumulate discrete materials through layer-by-layer printing in three dimensions under pre-defined design and precise control. Typically, this can be achieved through a software-layered discrete model and numerical control robotic printing system. The computer software generates several 2D planes by plating the 3D model, and the robotic printer applied laser beams, electron beams, hot melt nozzles, UV light, and other methods to stack these 2D planes and bond these layers to form a final product [13]. At present, 3DP technology has been applied to many fields such as construction, materials, the chemical industry, and aerospace [14, 15].

Among various 3DP techniques, fused deposition modeling (FDM) printing has been one of the popular printing methods [16]. It follows an STL file generated by computer-aided design (CAD) software, and the printing nozzle heat and melts the filament material to print the layer structures on the worktable. Compared with other molding technologies, FDM is an easy process, user-friendly, low maintenance, and has no foul or toxic gas emission [17]. The hot melt extrusion method (HEM) is to load the drug into the carrier to form a solid dispersion and so on [18]. In this method, the drug, polymer, and other auxiliary materials (such as plasticizers and release regulators) are thoroughly mixed and then heated and extruded by a hot extruder to produce a drug-containing polymer wire for FDM 3DP. HME does not require the use of high-concentration solvents, which improves the printing efficiency and can adjust the drug release characteristics by changing the shape, changing the printing polymer material, and changing the printing formulation [19].

This article is to investigate a new method for preparing controlled-release agents for field-specific or insect-specific pesticides by applying additive manufacturing technology to overcome these shortcomings of nano-carrier formulations. Its application includes any personalized needs or delicate landscapes such as fish tanks, decorative pools.

2. Materials and Methods

2.1. Experimental Materials

Acetaminophen (APAP) was used as a pesticide model drug, purchased from Belka Pharmaceutical Company, Wuhan, China. Poly ε-caprolactone (PCL) was purchased from Xinfu Industrial Co., Ltd., Shandong, China, and edible corn starch was purchased from Fuji Food Co., Ltd., Japan. Hydroxypropyl methylcellulose (HPMC) was purchased from Huizepu Pharmaceutical Technology Company, Hubei, China, and hydrochloric acid (12 mol/L) was purchased from Changpeng Chemical Co., Ltd, Chongqing, China. The water used in the experiment was deionized.

2.2. Preparation of Drug-Loaded Filament

After the PCL powder was sieved with a 100-mesh sieve, placed in a blast drying box (model 101-1AB, Beijing Zhongxing Weiye Century Co., Ltd.), set at a temperature of 30°C, and dried for 10 hours. Similarly, APAP, HPMC, and starch were screened using a 100-mesh sieve and dried at a temperature of 60°C for 6 hours. Physically mixes (PCL/APAP/starch or HPMC) were prepared according to Table 1.

Table 1. *Formulation of composite materials.*

Formula	PCL Wt.%	APAP Wt.%	HPMC Wt.%	Starch Wt.%
5/5/0	50	50	0	0
4/5/1HPMC	40	50	10	0
3/5/2HPMC	30	50	20	0
2/5/3HPMC	20	50	30	0
4/5/1Starch	40	50	0	10
3/5/2Starch	30	50	0	20
2/5/3Starch	20	50	0	30

They were separately fed into the extruder (model 3Dpany, Hongtu Machinery Equipment Factory, Erqi District, Zhengzhou City) and melt mixed to make a diameter of 1.75mm filaments with a nozzle temperature of 72°C. PLC was selected as the carrier material in the model drug-controlled release system due to its low melting point (around 60°C), as well as its good biodegradability, non-toxicity, and environmental friendliness. To increase the release rate of the system, water-soluble starch or hydrophilic HPMC was added to promote the increase of pores in the system to control the release behavior of the drug.

2.3. 3DP of Model Tablets

The 3DP tablet model was modeled with OpenSCAD version 2021.01, saved in STL format, and imported into Repetier-Host version 2.2.2, and then the prepared filaments were loaded into the 3D printer (CoreXY, Wuhu Senlang Electronic Technology Co., Ltd., China) and connected to the computer. The working temperature is 170°C, the printing speed is 10mm/s, and the temperature of the hotbed for forming the object was set at 25°C. It was planned to print different proportions of the formula, observed the molding effect, and modified the process parameters such as the printing layer height, retraction speed, etc., to improve the completeness and printability of the model tablet. More details are reported in the results and discussion section.

2.4. Fourier Infrared Spectroscopy (FTIR)

The infrared spectrum was used to monitor the loading of model drug APAP and evaluate the potential interaction between the model drug and the drug-loaded material (PCL), as well as the drug release regulator (water-soluble starch or HPMC) after 3DP. FTIR infrared spectrograms were taken in

the 400-4000 cm^{-1} using a TENSOR 27 Fourier transform infrared spectrometer (Bruker, Germany) by using attenuated total reflection mode.

2.5. X-ray Diffraction (XRD)

X-Ray structure analysis and determination of crystallinity of powder materials and 3DP tablets were performed using a DX-2600 X-Ray diffractometer (Fangyuan Instrument Co., Ltd., Dandong, China) with CuKα1 radiation and λ = 1.5418 Å. The intensity and voltage applied were 15 mA and 40 kV, respectively. The measurements were collected over a range of 2θ from 5° to 55° with a stepwise size of 0.05° at a speed of 5°/min. Scan to get the data and draw the X-ray diffraction pattern.

2.6. Thermal Analysis

A differential scanning calorimetry (DSC) 200 F3 Phoenix (Netsch GmbH, Germany) was used to study the crystallinity of the composites and to characterize the miscibility of the extrudates for analysis. Around 7 mg sample was sealed in an aluminum pan with a perforated lid, and the temperature was increased from 25°C to 200°C at a rate of 10 °C/min under a nitrogen purge of 100 mL/min. The software used for the DSC measurements was Proteus ver. 5.2.1 (Netsch GmbH, Germany). Thermogravimetric analysis (TGA) was conducted on STA409PC Synchronous thermal analyzer (Netsch GmbH, Germany). Powders and 3DP objects with around 10 mg were heated at 10 °C /min in open aluminum pans using nitrogen as a purge gas of 100 mL/min. Data collection and analysis were performed using Proteus ver. 5.2.1 (Netsch GmbH, Germany).

2.7. Scanning Electron Microscope (SEM)

The surfaces of the extruded filaments and 3DP tablets were imaged by scanning electron microscopy. Before imaging, all samples were fixed with double-sided carbon tape, and platinum sputter coating was performed with an SBC-12 ion sputterer (KYKY, Beijing, China) for 1 min. SEM images were then acquired using a VEGA 3 SBU (TESCAN, Czech) at 20 kV.

2.8. Drug Dissolution Test

The drug dissolution tests were to simulate the accelerated dissolution of the tablets in the natural environment. The experiment adopts the paddle method of the dissolution test described in the 2015 edition of the Chinese Pharmacopoeia (0931). The same batch of 3DP tablets was tested in an RC-6 dissolution tester (Tianjin Optical Instrument Factory, China). Each experiment was carried out at 37±0.5°C, and 1000mL of pH 1.0 dilute hydrochloric acid solution and pH 7.5 deionized water was used to simulate acidic and neutral moist soils, respectively. Each tablet was repeated in three groups under the same parameters. The paddle was positioned 15±1 mm away from the bottom of the dissolution tank, and the stirring speed was set to 100±1rpm. During the test, a sample of 5 mL was taken at 10, 30, 60, 120, 240, 360, 480, 600, and 720 minutes intervals. After cooling to room temperature, 254nm UV light on an i3 ultraviolet-visible spectrophotometer (Jinan Haineng Instrument Co., Ltd., China) was used to determine the absorbance. The absorbance is measured against a standard absorbance-concentration curve of APAP in the concentration range of 1-15mg/L. This standard curve under a pH=7.5 neutral environment shows A=43.152C+0.00008 (R^2=0.9999), and the standard curve under pH=1.0 acidic environment shows A=41.653C+0.0142, (R^2=0.9995). The dissolved APAP concentration and the drug release rate at different sampling time points can then be calculated according to these standard curves using equation (1). Here the Q(%) is the cumulative drug release percentage at each time interval, n represents the n^{th} sampling, C_n is the concentration of the nth sampling, V_0 is the volume of the dissolution liquid sampled each time that is 5mL, and M is the theoretical drug content. Since the proportion of APAP in all formulations is 50wt.%, we believe that the theoretical drug content M is 50% of the weight of a single 3DP tablet, as expressed in (2).

$$Q(\%)=\frac{C_n\times[1-(n-1)\times V_0]+(C_1+C_2+\ldots+C_{n-1})\times V_0}{M}\times 100 \quad (1)$$

$$M=\text{Single tablet weight}\times 50\% \quad (2)$$

2.9. Drug Release Profile Kinetics

The experimental data of in vitro cumulative dissolution was fitted to four mathematical models including zero-order (3), first-order (4), Higuchi (5), and Korsmeyer–Peppas model (6). The correlation coefficient (R^2) was used to evaluate which mathematical model the release behavior of the drug was closer to.

$$Q_t/Q_\infty = k \quad (3)$$

$$Q_t/Q_\infty = 1-e^{-kt} \quad (4)$$

$$Q_t/Q_\infty = k_H t^{\frac{1}{2}} \quad (5)$$

$$Q_t/Q_\infty = kt^n \quad (6)$$

Among them, Q_t and Q_∞ are the cumulative releases of the drug at time t, and ∞, respectively; k is the rate constant, and n is the release index.

3. Results and Discussion

In previous studies, encapsulation of pesticides in PCL nanocapsules has been shown to resist the decomposition of drugs by environmental factors to a certain extent and to prolong the duration of drug effect on the environment [20]. However, there is also a risk of inhalation of such nanoparticles into the lungs [21]. In another study, PCL and alginate were combined into hydrogel beads as a slow-release carrier and the drug release in the dry and rainy seasons was coped with by changing the size of the

gel beads [22], but there were also disadvantages of the tedious and complicated preparation process and inflexible size control. By summarizing the previous work, this study utilizes the characteristics of PCL combined with 3D printing to provide a novel and even at-home manufacturing method for slow-release pesticides. This slow-release pesticide has more flexibility in the delivery rate and can be molded into any shape of delivery system to accommodate the release of drugs with different potencies. The method focuses on applications for disease prevention or fertilizer application in indoor micro landscapes.

3.1. Preparation of Drug-Loaded Filament

Instead of a pack and load test, this study is based on the HME method to prepare drug-loaded filaments and to realize the controlled release of a drug. Therefore, the control of the extrusion temperature, cooling, and weight of drug-loading materials is the key to a smooth filaments extrusion. The melting point of the drug-polymer-regulator mixture system will be different from that of the pure polymer or pure drug. Also, it is important to make sure the even mixing of PCL and APAP and the melt PCL could uniformly encapsulate the dispersed drug. Table 2 shows the extrusion parameters of different PCL/APAP compositions with HPMC or starch.

Table 2. *Some information on the different formulations in HME.*

PCL/APAP/(HPMC or starch)	Extrusion nozzle temp °C	Extrusion speed mm/s	Filament diameter mm	Smooth-ness
5/5/0	74	161	1.59±0.02	Rough
4/5/1HPMC	72	155	1.52±0.01	Smooth
3/5/2HPMC	72	140	1.52±0.02	Smooth
2/5/3HPMC	72	*	*	*
4/5/1Starch	72	155	1.50±0.01	Smooth
3/5/2Starch	72	110	1.48±0.01	Smooth
2/5/3Starch	72	*	*	*

* Formulas failed to be extruded.

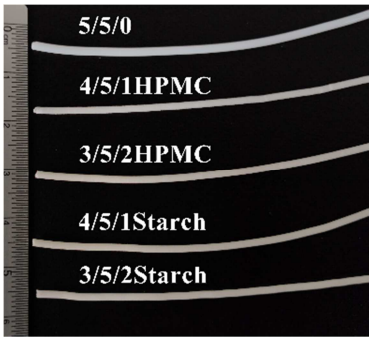

Figure 1. *Filaments of different formulations manufactured by HME.*

The screw extrusion speed was set to 5 rpm and the extrusion temperatures of 70°C, 72°C, 74°C, 80°C, and 90°C. It was found that at 72°C, the filaments of most formulations had a smoother and straighter appearance. One can see that any lower or higher extrusion temperatures resulted in a rough filament surface or may even clog the extrusion nozzle. Figure 1 demonstrated that with the increase of excipients, the color of the filament gradually turns yellow. The possible cause is the gelatinization of starch at high temperatures [23]. Table 2 summarizes the outcomes of each test and most filament products were of good quality. The extrusion speed was reduced to accommodate the increased resistance of the drug and excipient portion with the lower PCL content. In addition, the filament diameter decreased too, which may be related to the expansion rate of PCL material.

3.2. Determining the Printing Parameters

The model drug was designed with a thickness of 0.6mm for the shell and the middle infill cross (Figure 2). The diameter of the round tablet has a radius of 4mm and a height of 4mm. The top and bottom of the model were not capped to increase the surface area to improve the dissolution rate. Exported the model built in OpenSCAD into STL format, and then loaded it on Repetier-Host for slicing. The main 3dp parameters are shown in Table 3.

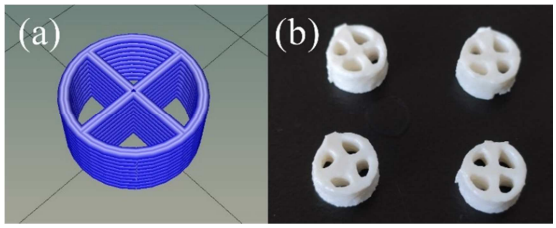

Figure 2. *(a) Tablet digital model in STL format, (b) Batch printed 3DP tablets.*

Table 3. *Main 3D printing process parameters.*

Parameters	Printing Temp. °C	Hotbed Temp. °C	Printing speed mm/s	Filament diameter mm
	170	25	15	1.55
Parameters	Layer height mm	Nozzle diameter mm	retraction speed mm/s	retraction distance mm
	0.3	0.4	0	0

Since the thickness of the model itself is only 0.6mm, and the nozzle diameter of the printer is 0.4mm, the infill density in the 3DP parameters should not play a major role. Therefore, it would be safe to ignore the influence of the

infill density.

However, the printing temperature will have a big impact on the printing quality. Experiments were designed with a printing temperature range of 150°C to 180°C at an increment of 5°C. Results showed an optimal printing temperature is at 170°C. Such higher is needed for the PCL composite materials to reach a sufficient higher temperature to have a fluidity for printing. If the printing temperature was too low (<165°C), the filament is unevenly melted and might clog the extrusion. However, if the printing temperature was too high (>175°C), it might cause starch carbonization and turn black and again block the nozzle. This situation became worsen when the PCL mass fraction was reduced. Furthermore, the higher the printing temperature, the softer the filament becomes. This will cause the extruder drive gear to lose the driving grip and its ability to drive the filament to the feeder. The reduced PCL content may result in insufficient bonding of the filament. As a result, the 3/5/2Starch formulation of filament could not be printed.

Printing speed is also a major factor affecting printing quality and printing efficiency. High printing speeds (20-30mm/s) will result in faster extrusion gear rotation and curled filament as shown in Figure 3. When the printing speed was too low (<10mm/s), the extrusion gear could not provide enough thrust to drive the filament. This would likely cause the nozzle to fail to extrude and clog. The optimal printing speed is set at 15mm/s to balance the thrust, the mechanical strength of the partially molten filament, and the resistance for smooth extrusion.

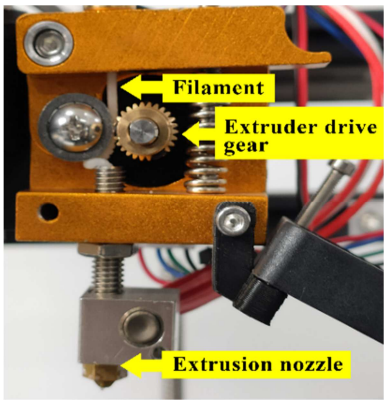

Figure 3. *Filament curls due to fast printing.*

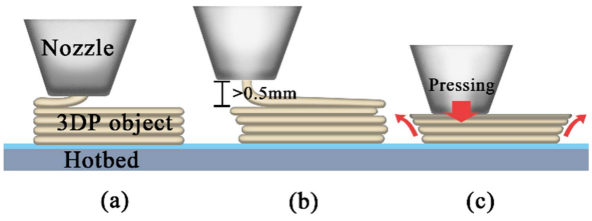

Figure 4. *(a) Schematic of the print head area, (b) Higher layer height results in low-quality 3DP object, (c) Lower layer height leads to nozzle squeezing of 3DP object.*

The layer height of the 3DP digital model is determined by printing steps and the model height which affects the compactness of the 3DP objects. When the layer height (<0.35mm) was smaller than the nozzle diameter (0.4mm), an inter-layer squeeze might occur and cause the deformation of the 3DP object (Figure 4c). However, when the layer height was set too big (>0.5 mm), the newly extruded filament failed to bound and fuse correctly with the previous layer [24], as shown in Figure 4 (b). Finally, an optimal layer height of 0.45mm was set to ensure the integrity and aesthetics of the 3DP tablets.

Last but not least printing parameters are the retraction speed and retraction distance. The retraction is necessary to reverse the extrusion gear after printing each track, pulling the filament out of the throat tube by applying a negative pressure. This will prevent the fused material from overflowing or dropping when the printing head is positioned in a new location or switching to a new printing pattern. However, the throat pipe in this work was designed for a 1.75mm diameter filament, a mismatch with the 1.48~1.60mm diameter filaments produced in this study. This caused the filament diameter to be stretched and becomes thinner after the retraction occurs. When the printing resumed, the filament strength was weakened and unable to drive the printing properly as shown in Figure 5. The alternative solution is to disable the retraction and manually remove the excess melt filament. Therefore, it is important to have consistent filament diameter and throat pipe diameter.

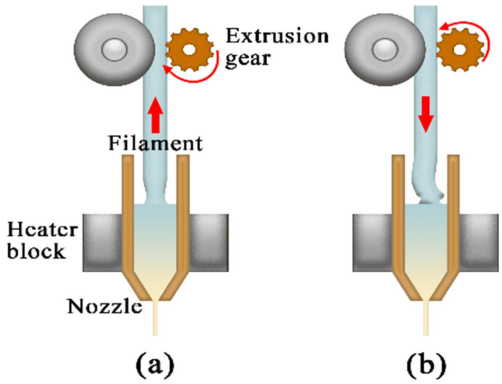

Figure 5. *(a) Back pumping causes the filament to stretch and become thin, (b) Feed again and the filament bends.*

3.3. Physical Characterization

To understand the interactions among components in the PCL composite materials, the FTIR of the pure substances and their printed tablets were collected (Figure 6). APAP showed hydroxyl stretching vibration at 3323 cm^{-1}, C=O stretching vibration absorption peak at 1656 cm^{-1}, and N-H amide stretching vibration at 1546 cm^{-1} [25]. PCL has the C-H symmetric stretching vibration absorption peak at 2944 cm^{-1}, CH_2 asymmetric stretching at 2865 cm^{-1}, and the C=O stretching vibration at 1726 cm^{-1} [26]. For starch and HPMC, both have a wide absorption band between 3500 and 3300 cm^{-1} which indicated hydrogen-bonded OH group and the absorption peak of C-H stretching vibration is at 3000-2500 cm^{-1} [27, 28]. All representative peaks of each respective pure

substance still appeared intact in the spectra, of the composite, which indicates the physical blending of PCL, the APAP drug and release regulators in the 3DP tablets. After heating and extrusion, no new chemical bonds or new substance was formed.

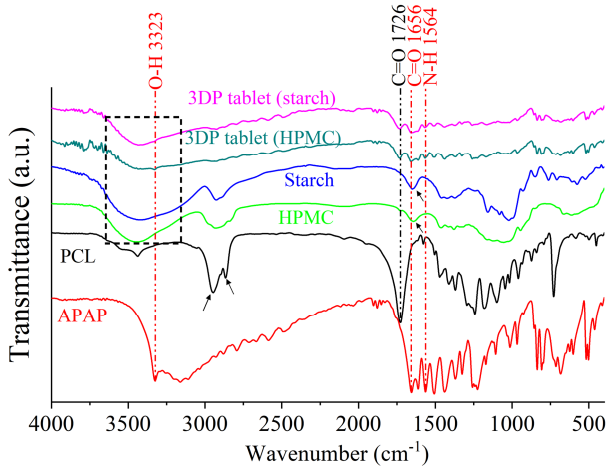

Figure 6. *IR spectra of single formulation raw materials, powder mixtures, and 3DP tablets.*

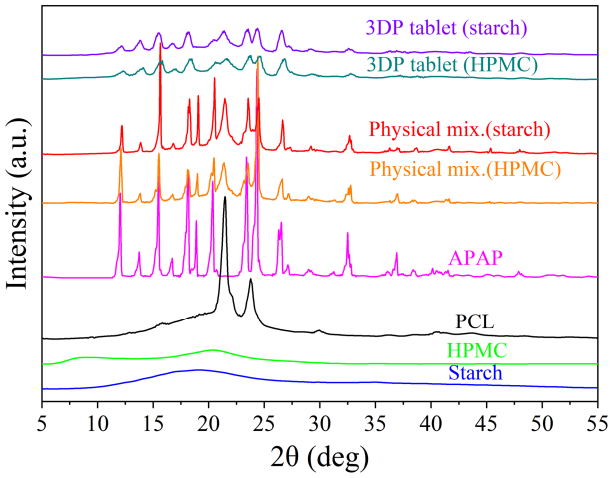

Figure 7. *X-ray diffraction patterns of single formulation raw materials, powder mixtures, and 3DP tablets.*

To explore the crystallinity of each component in the model drug, the X-ray diffraction (XRD) of the pure materials, their physical mixtures, and the 3DP tablets were collected (Figure 7). Again, no new characteristic peaks of HPMC and starch were found, which indicates the amorphous nature of these components. XRD of APAP showed peaks at 12.05, 15.50, 18.15, 20.34, 23.42, and 24.35 degrees, and PCL peaks at 21.48 and 23.78 degrees. The sharp peaks indicate excellent crystallinity and large crystal grains. The semi-crystalline polymer PCL has two distinct characteristic diffraction peaks, and the crystal content is relatively high. There are still multiple sharp Bragg peaks in their physical mixture [26], but there are no sharp diffraction peaks in the 3DP tablets, the peaks are broadened, and the peak heights are significantly lower. This suggested that the high-temperature melting of PCL during the HME method and 3DP process affected the arrangement of PCL molecular chains to some extent and reduced its crystallinity, which also partially transformed APAP into an amorphous phase.

DSC analysis (Figure 8) shows an endotherm melting peak at 67°C for PCL and 174°C for APAP. In contrast, HPMC and starch show no distinguish peaks, indicating a lower degree of crystallization. Interestingly, the DSC peak of 3DP tablets with HPMC and starch formulations both show two heat-absorbing peaks at 56°C and 164°C, respectively. Not only the temperature was ~10°C lower than the PCL and APAP peaks, but also the peak profile is not as sharp or well-defined as the pure substance. This suggests that PCL and APAP become amorphous after HME and 3DP [29].

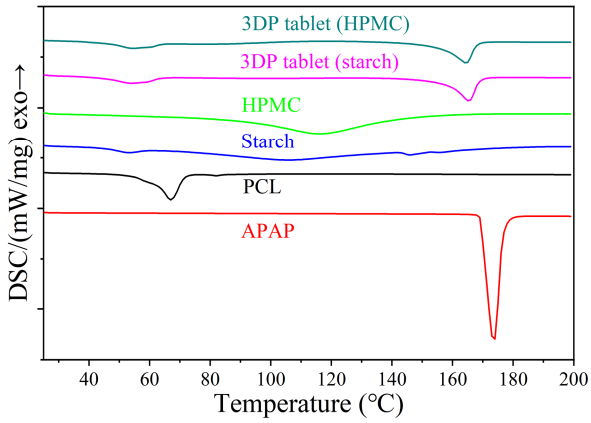

Figure 8. *DSC analysis of single formulation raw material, 3DP tablet.*

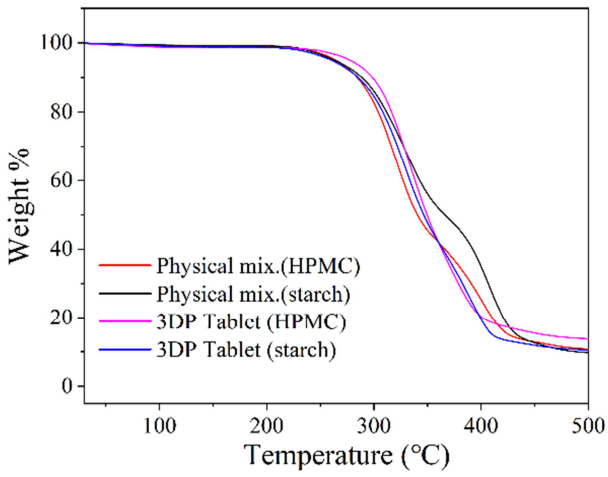

Figure 9. *TGA analysis of powder mixture, 3DP tablet.*

Thermogravimetric analysis TGA was used to gauge the thermal stability of the 3DP tablets. Figure 9 shows the similar TGA profiles of the two physical mixtures and the corresponding 3DP tablets. The steepest weight loss occurred between 250 and 300°C. The weight loss continues until about 400°C. The heating temperature of the 3DP process is 170±0.5°C where the weight loss is less than 1.3% (w/w). This weight loss probably is the loss of absorbing moisture from the air. During the 3DP process, the passing through the filament is relatively short (<1min) and stays at the heated nozzle

region at 170°C for a very short time. The extrusion will cool quickly after leaving the nozzle. Therefore, it is safe to ignore the weight loss in the final 3DP tablet.

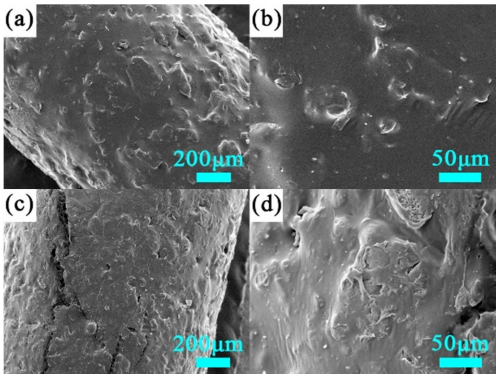

Figure 10. *SEM images of filament with formulation 4/5/1HPMC (a)(b) and formulation 3/5/2HPMC (c) (d).*

SEM was used to evaluate the microscopic morphology of the filament and 3DP tablets manufactured by the HME method. Figure 10 shows the surface of filaments formulated with 4/5/1HPMC and 3/5/2HPMC. While both SEM images reveal many irregular bumps, which could be attributed to inadequate PCL melting, the filament with 10 wt.% HPMC content was slightly smoother and flatter. In contrast, the surface of the filament with 20 wt.% HPMC had a long crack and was rougher. The 20 wt.% HPCM showed more large agglomerated structures. These bumps in PCL could be caused by APAP clumps and release regulators with moisture. The reduced PCL content resulted in insufficient bonding, increased cracks, and will result in a decreased ability to disperse the drug evenly.

Figure 11 further shows the microscopic morphology of 3DP tablets formulated with 4/5/1 HPMC before testing in an acidic environment at pH 1.0. It can be seen that the tablets made of 3DP have obvious print marks on the outer wall layer. However, 4/5/1 HPMC has good adhesion between the layers, uniform layer height, and no fracture or obvious defects. The 500x view (Figure 11c) shows a large number of coral-like cracks and small holes smaller than 5 μm on the surface. This was most likely caused by the shrinkage of the molten PCL material upon cooling. This coral-like structure could serve as a good pathway for the dissolution and controlled release of internal drugs.

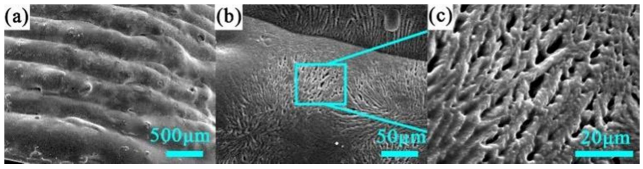

Figure 11. *SEM images of 3DP tablet with formulation 4/5/1HPMC at different magnifications.*

3.4. Drug Dissolution Test

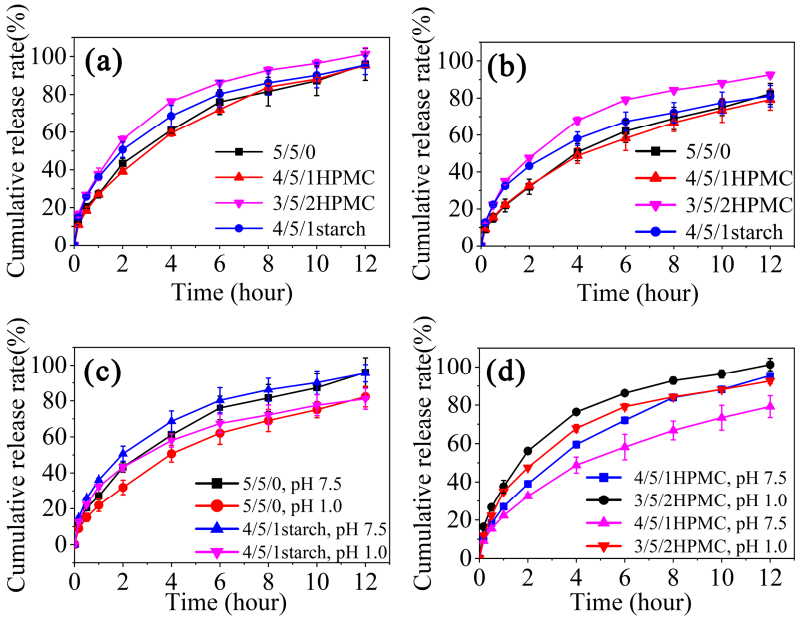

Figure 12. *Dissolution profiles of different formulations of 3DP tablets in pH 7.5 (a) and pH 1.0 (b) environments. Comparison of dissolution profiles of 3DP tablets formulated with 5/5/0 and 4/5/1 starch in different environments (c). Comparison of dissolution profiles of 3DP tablets with 4/5/1 HPMC and 3/5/2 HPMC in different environments (d).*

Figure 12 shows the drug dissolution test results of 5/5/0, 4/5/1HPMC, 3/5/2HPMC, and 4/5/1starch. Figure 12a is under pH=7.5 and Figure 12b is in an acidic solution pH=1.0. One can see that 3DP tablets with either release regulator formulation achieved a cumulative dissolution rate of more than 80% within 12 hours in both neutral and acidic environments, as shown in Figure 12 (a) (b). For example, the cumulative dissolution of 3/5/2HPMC in the neutral environment was 95.81% while the other three composites show 94.41%. The corresponding cumulative dissolution in the acidic environment was 82.31%

and 79.22%, respectively. One can see that the overall dissolution rate in the neutral environment is more than 10% higher than those in the acidic environment. The 3DP tablets of both 3/5/2HPMC (pink line in Figure 12a/b) and 4/5/1 starch (blue line in Figure 12a/b) formulations had faster release rates in the first 1 hour, reaching 50% cumulative release than those of 5/5/0 (black) and 4/5/1HPMC (red). In contrast, the dissolution profiles of 5/5/0 and 4/5/1HPMC formulations revealed similar profiles and are lower than the 3/5/2HPMC and 4/5/1starch composite. This is an important observation because for the same ratio of formulations, starch as a release regulator had a higher release rate than HPMC in both environments. This provides a new design approach in 3DP formulations by adjusting the release regulator content and type to meet and alter the controlled-release needs.

To compare the cumulative dissolution between the acidic and neutral environment, Figure 12c shows the 5/5/0 and 4/5/1starch profiles and Figure 12d shows HPMC profiles. It is interesting to note that both Figure 12c/d shows the cumulative drug release in a neutral environment was higher than in those in an acidic environment. This is probably because APAP itself is a weak acid and dissolution equilibrium would favor a neutral environment.

To simulate the kinetic model of the dissolution of 3DP tablets, the zero-order, first-order, Higuchi model, and Korsmeyer–Peppas model (equations 3-6) will be used to fit the above dissolution data. Table 4 and Table 5 summarize the correlation coefficients of different kinetic models for each dissolution profile in neutral and acidic environments, respectively. Most of the formulations had the highest R^2 for the Korsmeyer–Peppas model, indicating that the Korsmeyer–Peppas model is probably the most suitable to describe the 3DP drug release behavior. The Higuchi and Korsmeyer–Peppas models for 4/5/1HPCM in neutral and acidic environments had similar R^2 values. Their diffusion exponents n in the Korsmeyer–Peppas model (6) were 0.49802 ± 0.02009 and 0.49868 ± 0.01225, respectively. These diffusion exponent values were close to the release index of 0.5 in the Higuchi model (5), and n in the range of 0.45 to 0.89 indicated the release mechanism of anomalous transport [30]. Therefore, the diffusion of 4/5/1HPMC composite was more likely to be caused by a combination of Fick‘s diffusion and matrix erosion. HPMC transformed into a hydrogel and dissolved slowly, controlling the rate of drug diffusion and release, consistent with anomalous transport [29]. The Korsmeyer–Peppas model for both formulations 3/5/2HPMC and 4/5/1 starch had high R^2 values and n values below 0.45, indicating that their drug release behavior in both environments is dominated by Fick's diffusion. The decrease in wt.% of the PCL matrix might provide wider drug release channels during dissolution. The release of HPMC hydrogels further accelerates dissolution and leads to higher drug diffusion and release. On the other hand, the water-soluble starch could not form a similar HPMC hydrogel, therefore, its release closely follows Fick's diffusion law.

Table 4. *Statistical parameters of dissolution profiles of 3DP tablets fitting with different kinetic models in a neutral environment.*

Formula	Zero-Order R^2	First-Order R^2	Higuchi R^2	Korsmeyer–Peppas	
				R^2	n
5/5/0	0.913	0.972	0.989	*0.991*	0.467
4/5/1HPMC	0.927	0.979	0.994	*0.994*	0.498
3/5/2HPMC	0.843	0.971	0.962	*0.978*	0.387
4/5/1Starch	0.863	0.962	0.973	0.986	0.393

Table 5. *Statistical parameters of dissolution profiles of 3DP tablets fitting with different kinetic models in an acidic environment.*

Formula	Zero-Order R^2	First-Order R^2	Higuchi R^2	Korsmeyer–Peppas	
				R^2	n
5/5/0	0.933	0.981	*0.995*	0.994	0.513
4/5/1HPMC	0.938	0.973	0.998	*0.998*	0.499
3/5/2HPMC	0.849	0.978	0.966	*0.978*	0.410
4/5/1Starch	0.869	0.953	0.976	*0.990*	0.387

4. Conclusion

In summary, we have developed an intelligent environmentally responsive controlled-release pesticide formulation for pesticide transportation, pest control, and fertilization. Through a simple physical mixing and mature 3DP process, the simulated drug is loaded on a composite carrier with a biodegradable green material PCL material and a natural polymer material as a release regulator. The prepared simulated tablet is environmentally friendly, pollution-free, and can control and release drugs through the chemical environment change control compound carrier. In addition, compared with nanoparticles, emulsifiers, nano-crystals, etc., this 3DP tablet has higher drug loading, controllable drug loading, stable drug release ability, and certain UV shielding performance, and the manufacturing process is simple. There is no need for expensive and special equipment to participate, which greatly reduces production costs and simplifies the production process, which is of great significance to the practical application of pesticides. Therefore, the development of intelligent environmentally sensitive pesticide formulations for agricultural pests and diseases is feasible. It has the potential to improve the efficacy of pesticides and reduce the number of pesticides and has broad practical application prospects.

Acknowledgements

HJSF would like to acknowledge the partial financial support from the Science Foundation of Sichuan University of Science & Engineering (2020RC06) and the Natural Science Foundation of Sichuan Province (SYZ202133 & 2022JDGD0041). The authors would like to thank the College of Chemical Engineering at Sichuan University of Science and Engineering for providing the lab facility and logistic support for this project.

References

[1] Raileanu, M., et al., Sol-gel materials with pesticide delivery properties. Journal of Environmental Protection, 2010. 1 (03): p. 302.

[2] Hao, L., et al., Composite pesticide nanocarriers involving functionalized boron nitride nanoplatelets for pH-responsive release and enhanced UV stability. Chemical Engineering Journal, 2020. 396: p. 125233.

[3] Knowles, A., Recent developments of safer formulations of agrochemicals. The Environmentalist, 2008. 28 (1): p. 35-44.

[4] Pan, B., et al., Comparative efficacy of oil solution and wettable powder of lambda-cyhalothrin to naturally occurring Ornithonyssus sylviarum infestation of chickens. Veterinary parasitology, 2009. 164 (2-4): p. 353-356.

[5] Massinon, M., et al., Spray droplet impaction outcomes for different plant species and spray formulations. Crop Protection, 2017. 99: p. 65-75.

[6] Nuruzzaman, M., et al., Nanoencapsulation, nano-guard for pesticides: a new window for safe application. Journal of agricultural and food chemistry, 2016. 64 (7): p. 1447-1483.

[7] Cui, B., et al., Emamectin benzoate-loaded zein nanoparticles produced by antisolvent precipitation method. Polymer Testing, 2021. 94.

[8] He, F., et al., Fabrication of a sustained release delivery system for pesticides using interpenetrating polyacrylamide/alginate/montmorillonite nanocomposite hydrogels. Applied Clay Science, 2019. 183.

[9] Septiyanti, M., Evaluation of Nanoemulsion Concentrate Botanical Fungicide from Neem, Citronella and Eugenol Oil Using Palm Oil Based Surfactant. American Journal of Physics and Applications, 2019. 7 (1).

[10] Wang, Y., et al., A new temperature-responsive controlled-release pesticide formulation – poly (N-isopropylacrylamide) modified graphene oxide as the nanocarrier for lambda-cyhalothrin delivery and their application in pesticide transportation. Colloids and Surfaces A: Physicochemical and Engineering Aspects, 2021. 612.

[11] Vega-Vasquez, P., N. S. Mosier, and J. Irudayaraj, Nanoscale Drug Delivery Systems: From Medicine to Agriculture. Frontiers in Bioengineering and Biotechnology, 2020. 8.

[12] Oztemel, E. and S. Gursev, Literature review of Industry 4.0 and related technologies. Journal of Intelligent Manufacturing, 2018. 31 (1): p. 127-182.

[13] Mohammed, A., et al., Additive Manufacturing Technologies for Drug Delivery Applications. Int J Pharm, 2020. 580: p. 119245.

[14] Ligon, S. C., et al., Polymers for 3D Printing and Customized Additive Manufacturing. Chem Rev, 2017. 117 (15): p. 10212-10290.

[15] Chen, Z., et al., 3D printing of ceramics: A review. Journal of the European Ceramic Society, 2019. 39 (4): p. 661-687.

[16] Araujo, M. R. P., et al., The Digital Pharmacies Era: How 3D Printing Technology Using Fused Deposition Modeling Can Become a Reality. Pharmaceutics, 2019. 11 (3).

[17] Mazzanti, V., L. Malagutti, and F. Mollica, FDM 3D Printing of Polymers Containing Natural Fillers: A Review of their Mechanical Properties. Polymers (Basel), 2019. 11 (7).

[18] Bandari, S., et al., Coupling hot melt extrusion and fused deposition modeling: Critical properties for successful performance. Adv Drug Deliv Rev, 2021. 172: p. 52-63.

[19] Pereira, G. G., et al., Polymer Selection for Hot-Melt Extrusion Coupled to Fused Deposition Modelling in Pharmaceutics. Pharmaceutics, 2020. 12 (9).

[20] Peres, M. C., et al., In natura and nanoencapsulated essential oils from Xylopia aromatica reduce oviposition of Bemisia tabaci in Phaseolus vulgaris. Journal of Pest Science, 2020. 93 (2): p. 807-821.

[21] Moore, A. J. S., et al., Bioreactivity of a novel poly (epsilon-caprolactone) nanocapsule containing atrazine with human lung alveolar epithelial cells. Environmental Science: Nano, 2022. 9 (6): p. 2134-2148.

[22] Mun, A., et al., Alginate hydrogel beads embedded with drug-bearing polycaprolactone microspheres for sustained release of paclobutrazol. Sci Rep, 2021. 11 (1): p. 10877.

[23] Dai, Y., et al., Determination of starch gelatinization temperatures by an automated headspace gas chromatography. Journal of Chromatography A, 2019. 1602: p. 419-424.

[24] Elbl, J., J. Gajdziok, and J. Kolarczyk, 3D printing of multilayered orodispersible films with in-process drying. International Journal of Pharmaceutics, 2020. 575.

[25] Rodriguez-Pombo, L., et al., Volumetric 3D printing for rapid production of medicines. Additive Manufacturing, 2022. 52.

[26] Yang, Y., et al., 3D-printed polycaprolactone-chitosan based drug delivery implants for personalized administration. Materials & Design, 2022. 214.

[27] Sethi, S., et al., Cross-linked xanthan gum-starch hydrogels as promising materials for controlled drug delivery. Cellulose, 2020. 27 (8): p. 4565-4589.

[28] Tedesco, M. P., et al., Production of oral films based on pre-gelatinized starch, CMC and HPMC for delivery of bioactive compounds extract from acerola industrial waste. Industrial Crops and Products, 2021. 170.

[29] Fina, F., et al., 3D Printing of Tunable Zero-Order Release Printlets. Polymers (Basel), 2020. 12 (8).

[30] Costa, P. and J. M. Sousa Lobo, Modeling and comparison of dissolution profiles. European Journal of Pharmaceutical Sciences, 2001. 13 (2): p. 123-133.